Particle formation and aggregation–collapse behavior of poly(*N*-isopropylacrylamide) and poly(ethylene glycol) block copolymers in the presence of cross-linking agent

PENG-WEI ZHU
School of Physics and Materials Engineering, CRC for Polymers, Monash University, VIC 3800, Australia
E-mail: peng.zhu@spme.monash.edu.au

The effect of feed molar ratio of *N*-isopropylacrylamide (NIPAM) to poly(ethylene oxide) (PEO) on the particle formation of poly(*N*-isopropylacrylamide) (PNIPAM) and PEO block copolymers (PNIPAM-*b*-PEO) and their aggregation–collapse behavior have been studied in aqueous solutions. It is found that in the presence of cross-linking agent *N*,*N*′-methylenebisacryla-mide (BIS), different morphologies of PNIPAM-*b*-PEO copolymers can be obtained, including a grafting-like structure, a hemispherical core-shell structure and a well-defined core-shell nanoparticle, as the feed molar amount of NIPAM in the copolymerization is increased. The increase in temperature causes the self-aggregation of grafting-like copolymers and hemispherical particles due to the hydrophobic interaction between locally unshielded PNIPAM blocks prior to the conformational transition of PNIPAM. When the feed molar ratio of NIPAM to PEO exceeds a certain value, a well-defined core-shell nanoparticle can be produced during the copolymerization. At low concentrations, PNIPAM cores of single core-shell nanoparticles can undergo the conformational transition without aggregation. The increase in the concentration of the well-defined core-shell nanoparticles, however, results in a week aggregation at temperatures lower than the θ-temperature of pure PNIPAM due to the association of methyl groups at the periphery of PEO shells.

1. Introduction

Stimuli-responsive polymers and their corresponding gels have attracted much attention because they have many potential applications in numerous fields, including drug delivery [1], biomaterials [2], cell culture systems [3] and bioseparations [4]. Most of the above-mentioned materials were prepared from a limited number of synthetic polymers. Poly(*N*-isopropylacrylamide) (PNIPAM) is perhaps the most widely studied among temperature-responsive polymers [5, 6]. Pure PNIPAM chains dissolve in water at room temperature but exhibits a lower critical solution temperature (LCST) of 32 °C. The coil-to-globule transition of single PNIPAM chains can be observed at ∼ 32 °C if the PNIPAM aggregation is effectively prevented [5, 6]. The conformational change of single PNIPAM chain is considered to have similar characteristics to biological macromolecules, such as protein folding [7]. Materials containing PNIPAM as a building block can also undergo a reversible and controllable phase or conformational transition in response to external stimuli, such as temperature [8], pH [9], solvent composition [10], chemical component [11], biomaterials [12] and light [13].

Block copolymer microgels containing PNIPAM and poly(ethylene oxide) (PEO), PNIPAM-*b*-PEO, have recently been studied [14, 15]. Microgels are interesting because they can respond quickly to their environment in contrast to macroscopic gels [16]. Microgel nanoparticles formed from a self-aggregation of amphiphilic block copolymers have potential applications for self-assembled nanomaterials. In general, the self-aggregation of amphiphilic block copolymers depends on solvent quality, concentration and composition. Any change in the temperature, concentration and composition can result in selective solvent conditions under which thermodynamically stable copolymer particles with controlled structures and different morphologies may form. The θ-temperature of PEO was estimated to be 102 °C in pure water [17]. At lower temperatures, whether or not PEO chains can undergo aggregation in aqueous solutions is not clear [17–19]. There is no doubt, however, that the change with temperature from hydrophilic to hydrophobic occurs much more slowly for PEO chains than that for PNIPAM chains. This can consequently bring about a selective solvent condition only for PNIPAM blocks. The previous results reveal that for a very dilute solution of PNIPAM-*b*-PEO, the

increase in the number of hydrophilic PEO can lead to an increase in the critical aggregation temperature [15]. It is also found that the critical aggregation temperature is dependent of the concentration of copolymers.

Since the PNIPAM-*b*-PEO copolymers were synthesized by the copolymerization of NIPAM with poly(ethylene glycol) methyl ether (CH_3–$(OCH_2CH_2)_n$–OH) in the presence of a cross-linking agent [14, 15], the single PNIPAM-*b*-PEO particles formed under certain conditions should consist of a hydrophobic PNIPAM core and a hydrophilic PEO shell with hydrophobic methyl groups at the periphery of the PEO shell. The purpose of the present work is to investigate the influence of the feed molar ratio of NIPAM to PEO on the formation of PNIPAM-*b*-PEO particles in the presence of cross-linking agent *N*-*N*′-methylenebisacrylamide (BIS) and temperature-induced the aggregation–collapse behavior of PNIPAM-*b*-PEO.

2. Experimental part

Poly(ethylene glycol) methyl ether (CH_3–$(OCH_2CH_2)_n$–OH) from Aldrich, with an average number molecular weight of 5000, was dissolved in water and then the solution was filtered through a 0.45 μm Millipore filter. NIPAM from Monomer–Polymer was purified by a recrystalization in a 65/35 mixture of hexane and benzene. BIS and ceric ammonium nitrate from Aldrich were used as received. Details of the preparation of PNIPAM-*b*-PEO in the presence of BIS have been given in the previous work [15]. Typically, the poly(ethylene glycol) methyl ether (0.5 g) and NIPAM (0.42, 0.64, 1.28, 3.21 and 4.49 g) were dissolved in 40 mL of 1 N nitric acid solution at 50 °C. The feed molar ratios of NIPAM to poly(ethylene glycol) methyl ether were 34, 57, 114, 284 and 398. These block copolymers obtained were denoted as PNIPAM-*b*-PEO-*r* with *r* being the feed molar ratio of NIPAM to PEO. The solutions were stirred under a positive nitrogen pressure for 15 min and a solution of 7.24 g ceric ammonium nitrate in 10 mL of 1 N nitric acid was added. A solution of BIS in 10 mL of 1 N nitric acid was added with a feed molar ratio of BIS/NIPAM of 5.0×10^{-3} in $\sim$ 8 min after the addition of ceric ammonium nitrate solution. The copolymerization was continued at 50 °C for 6 h. The precipitation was observed during the copolymerization, especially for higher feed molar ratios of NIPAM to PEO. The solutions of precipitated copolymers were respectively dialyzed by repeated changes of fresh Milli-Q water at room temperature for one day and then at 5 °C for several days until the conductivity of pure Milli-Q water was achieved. The precipitated PNIPAM-*b*-PEO dissolved in water at the lower temperature and transparent solutions were finally obtained. No polymerization was found in a period of 6 h at 50 °C when a solution of ceric ammonium nitrate was added to a NIPAM solution in the absence of PEO.

The intrinsic stability of aqueous solutions of PNIPAM-*b*-PEO was carefully checked at 50 °C by repeated measurements of particle sizes. For very dilute solutions, the transparent solutions turned blue upon heating, indicating the formation of stable single particles or stable aggregate particles. The milky solutions were not observed at 50 °C after about 48 h. If the PNIPAM-*b*-PEO samples were not dialyzed throughout, a progressive precipitation occurred at 35 °C even though the aqueous solutions were very dilute. These results imply that residual $Ce^{(III)}$ ions produced during the copolymerization may interact with the copolymers or their aggregate particles to form insoluble complexes at higher temperatures.

Dynamic light scattering measurements were performed at 90° with an argon ion laser operating at a wavelength of 488 nm and at a power of 50 mW. The autocorrelation function was measured using a Malvern 4700c correlator. The average hydrodynamic radius $\langle R_h \rangle$ was determined using the Stokes–Einstein relation $\langle R_h \rangle = k_B T/(6\pi\eta D)$, where k_B, T, η and D are the Boltzmann constant, the absolute temperature, the solvent viscosity and the diffusion coefficient. The particle size distribution was obtained using a CONTIN program. The solutions were prepared by diluting a stock solution and then were filtered through 0.45 μm Millipore filter directly into a light scattering cell. The concentration of the microgels was calculated from the solid content after water evaporation. The solution temperature was controlled within $\pm$ 0.2 °C. The change in the solvent viscosity with temperature was taken into account in the dynamic light scattering experiments. The solutions were kept at each temperature at least for 10 min before dynamic light scattering measurements unless otherwise stated.

3. Results and discussion

Fig. 1 shows the temperature dependence of the average hydrodynamic radius $\langle R_h \rangle$ of PNIPAM-*b*-PEO-34 at a polymer concentration $c = 1.24 \times 10^{-3}$ g/mL. This concentration is higher than $c = 2.1 \times 10^{-4}$ g/mL at which the critical aggregation temperature of PNIPAM-*b*-PEO-34 is about 38 °C [15]. The accurate values of $\langle R_h \rangle$ were obtained only when the temperature was raised to 33 °C. Note that this temperature is the same as the LCST of pure PNIPAM. The average size of aggregate particles is almost a constant when the temperature is higher than about 50 °C.

Fig. 2 shows the temperature dependence of $\langle R_h \rangle$ of PNIPAM-*b*-PEO-57 at $c = 1.24 \times 10^{-3}$ g/mL. The critical aggregation temperature of PNIPAM-*b*-PEO-57 at

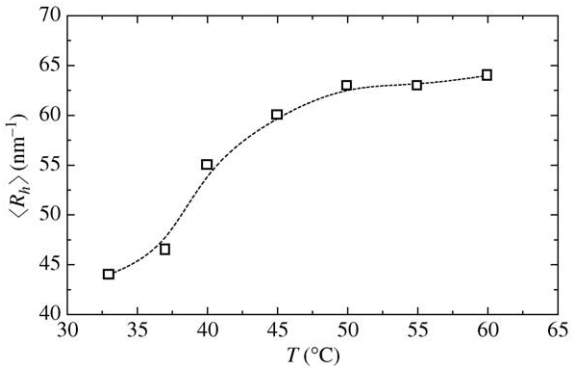

Figure 1 Temperature dependence of the average hydrodynamic radius $\langle R_h \rangle$ of PNIPAM-*b*-PEO-34 at $c = 1.24 \times 10^{-3}$ g/mL.

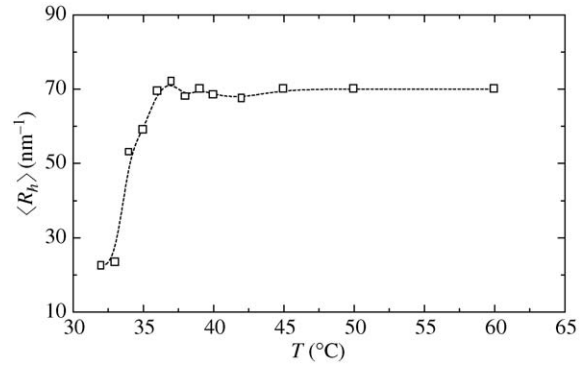

Figure 2 Temperature dependence of the average hydrodynamic radius $\langle R_h \rangle$ of PNIPAM-*b*-PEO-57 at $c = 1.24 \times 10^{-3}$ g/mL.

$c = 2.1 \times 10^{-4}$ g/ml is 35.5 °C [19]. Like PNIPAM-*b*-PEO-34, PNIPAM-*b*-PEO-57 also begins to undergo aggregation at 33 °C. However, the aggregation process of PNIPAM-*b*-PEO-57 is much faster than that of PNIPAM-*b*-PEO-34 and the average size of aggregate particles increases in a narrow range of temperature. The stable size of PNIPAM-*b*-PEO-57 aggregate particles is found to be larger than that of PNIPAM-*b*-PEO-34 over a wide range of temperature. It is worth noting that the average size of PNIPAM-*b*-PEO-57 aggregate particles reaches a maximum value at about 37 °C and then decreases slightly with a further increase in temperature. This phenomenon indicates a competition between aggregation of copolymers and collapse of stable aggregate particles. Despite the fact that the average size increases monotonously with temperature in a wide range, the collapse of PNIPAM blocks should occur inside the stable aggregate particles during the aggregation.

Fig. 3 shows the temperature dependence of $\langle R_h \rangle$ of PNIPAM-*b*-PEO-114 at the same concentration as shown in Figs. 1 and 2. It can be seen from Fig. 3 that $\langle R_h \rangle$ proceeds sequentially through several stages with increasing temperature. In the range 25–32 °C, $\langle R_h \rangle$ decreases slightly with increasing temperature, suggesting a weak contraction of PNIPAM blocks under better than θ-temperature condition, which is probably due to the dehydration of PNIPAM. PNIPAM-*b*-PEO-114 also starts to interact with each other at 33 °C. The value of $\langle R_h \rangle$ increases sharply with increasing temperature and reaches a maximum at 37 °C. As the temperature is increased from 38 to 40 °C, the average size of aggregate particles decreases significantly. A further increase in temperature does not cause a change in the average size of aggregate particles. It is found that the average size of stable PNIPAM-*b*-PEO-114 aggregate particles is smaller than that of PNIPAM-*b*-PEO-34 and PNIPAM-*b*-PEO-57, although the PNIPAM-*b*-PEO-114 contains more hydrophobic PNIPAM blocks. Note that all sizes of PNIPAM-*b*-PEO-114 aggregate particles are smaller than about 33 nm. This value is smaller than 50 nm that is generally accepted as an upper-limit radius of nanoparticles.

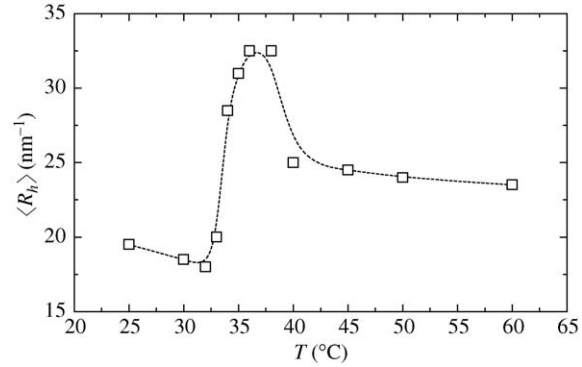

Figure 3 Temperature dependence of the average hydrodynamic radius $\langle R_h \rangle$ of PNIPAM-*b*-PEO-114 at $c = 1.24 \times 10^{-3}$ g/mL.

The results from Fig. 3 suggest that the fewer number of collisions between PNIPAM-*b*-PEO-114 would be sufficient to form stable core-shell nanoparticles in which a PNIPAM core is covered with a PEO shell, although the coexistence of PNIPAM and PEO blocks inside the aggregate particles cannot be totally ruled out. The decrease in $\langle R_h \rangle$ when $T > 37$ °C indicates a further collapse of loose PNIPAM globules inside the stable aggregate nanoparticles.

The competition between aggregation and collapse in PNIPAM-*b*-PEO-114 is also evident from the distribution of particle sizes. For a comparison, Fig. 4 shows two distributions of particle sizes of PNIPAM-*b*-PEO-34 and PNIPAM-*b*-PEO-114. At 33 °C, there is only one peak for both copolymers. However, unlike the size distribution of PNIPAM-*b*-PEO-34 aggregate particles, the increase in temperature brings about the formation of a bimodal distribution of PNIPAM-*b*-PEO-114 aggregate particles. The peaks at 15 and 62 nm would correspond to the average hydrodynamic radii of individual collapsed nanoparticles and aggregate particles, respectively. The

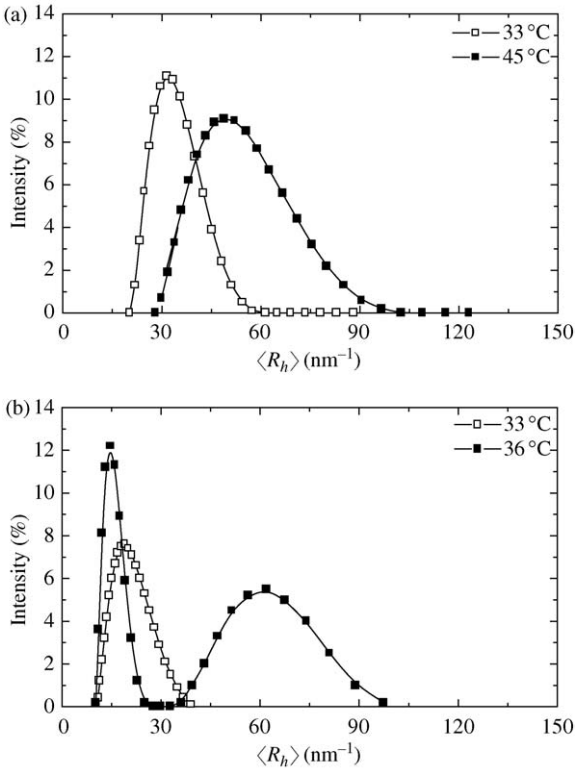

Figure 4 The average hydrodynamic radius distribution for (a) PNIPAM-*b*-PEO-34 and (b) PNIPAM-*b*-PEO-114 at $c = 1.24 \times 10^{-3}$ g/mL.

same behavior was also found in the PNIPAM grafted with PEO [20, 21].

The maximum $\langle R_h \rangle$ obtained from PNIPAM-*b*-PEO-114 aggregate particles is 33 nm at 37 °C. This size is smaller than 45 nm of PNIPAM-*b*-PEO-34 and 65 nm of PNIPAM-*b*-PEO-57 at the same temperature, although PNIPAM-*b*-PEO-114 contains the larger amount of more hydrophobic PNIPAM. The maximum values of volume ratio are estimated to be about 3.0, 30 and 5.0 in the range of temperature, corresponding to the feed molar ratios of 34, 57 and 114, respectively. The light intensity of PNIPAM-*b*-PEO-114 aggregate particles is found to be lower than that of PNIPAM-*b*-PEO-57. These findings seem to be contrary to the normal expectation that the higher amount of hydrophilic PEO block can more effectively prevent PNIPAM from undergoing aggregation.

A consistent interpretation of the aggregation–collapse behavior is given schematically in Fig. 5 with reference to the experimental data obtained. It is suggested that as the feed molar ratio of NIPAM to PEO is increased from 34 to 114, the morphology of PNIPAM-*b*-PEO formed during the copolymerization would presumably change from grafting-like into hemisphere-like with a heterogeneous and incoherent structure. As a consequence, the PNIPAM blocks in these copolymers would be locally in an unsheltered position. The fraction of exposed PNIPAM blocks is expected to be larger in PNIPAM-*b*-PEO-57 than that in PNIPAM-*b*-PEO-114, as shown schematically in Fig. 5. Once the temperature is raised, the more number of collisions among PNIPAM blocks of PNIPAM-*b*-PEO-57 are required to form a complete core-shell structure than those of PNIPAM-*b*-PEO-114. The average size of PNIPAM-*b*-PEO-57 aggregate particles is larger than that of PNIPAM-*b*-PEO-114, as observed in Figs. 2 and 3. In addition, a partial dehydration of solvated PNIPAM blocks with increasing temperature occurs to a certain extent under better than θ-temperature condition of pure PNIPAM. This can gradually weaken the degree of miscibility between contracted PNIPAM and solvated PEO, and consequently, pushes some of PNIPAM blocks into a more exposed position. At high temperatures, the cores of PNIPAM-*b*-PEO-57 and PNIPAM-*b*-PEO-114 aggregate particles are expected to comprise mainly of PNIPAM blocks, but PEO would affect the hydrophilic–hydrophobic balance in the cores to a certain extent. Note that there are a large number of methyl groups at the periphery of PEO shells. The local concentration of these methyl groups can be dramatically increased once the aggregation and collapse occur. The hydrophobic interaction between methyl groups would play a role in the formation of aggregate particles, although the details are not clear.

For PNIPAM-*b*-PEO-34, the decrease in the average size due to the PNIPAM collapse is too small to affect the overall dimension of aggregate particles. Although the stable aggregate particles should be sterically stabilized by PEO [22], it is expected that the stable aggregate particles of PNIPAM-*b*-PEO-34 could not be an individual core-shell structure as a whole but a mixture of small PNIPAM domains connected with PEO segments. Such aggregate particles have a low density of polymers and are filled with a lot of water molecules in the overall range of temperature studied.

As the feed molar ratio of NIPAM to PEO is increased further, different aggregation–collapse behavior is observed. Fig. 6 shows the temperature dependence of $\langle R_h \rangle$ of PNIPAM-*b*-PEO-284 and PNIPAM-*b*-PEO-398 at two concentrations of 1.24×10^{-3} and 2.47×10^{-4} g/mL. At $c = 1.24 \times 10^{-3}$ g/mL, unlike the aggregation–collapse behavior of the above copolymers, the average size of PNIPAM-*b*-PEO-284 decreases successively from 43 to 23 nm with increasing temperature. The same behavior is also found for PNIPAM-*b*-PEO-398 at the same concentration. The increase in the average size is not observed over the entire range of temperature.

The possible aggregation occurring in PNIPAM-*b*-PEO-284 and PNIPAM-*b*-PEO-398 at $c = 1.24 \times 10^{-3}$ g/mL is ruled out from the observation that the temperature dependence of $\langle R_h \rangle$ at a very dilute solution $c = 2.47 \times 10^{-4}$ g/mL exhibits the same fashion as that at $c = 1.24 \times 10^{-3}$ g/mL. No aggregation is also

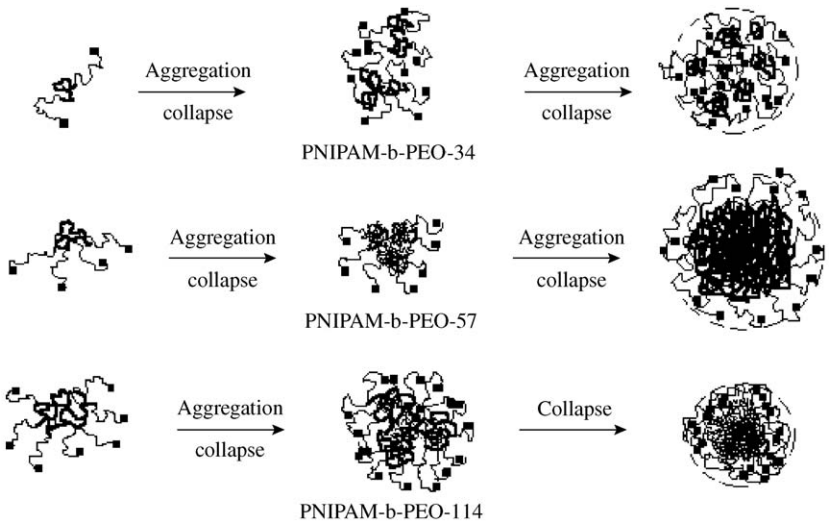

Figure 5 Schematic models for formation mechanisms of aggregate particles and collapse transition of PNIPAM-*b*-PEO with low feed molar ratios of NIPAM to PEO. Thin and bold curves represent PEO and PNIPAM, respectively. Filled squares represent methyl groups.

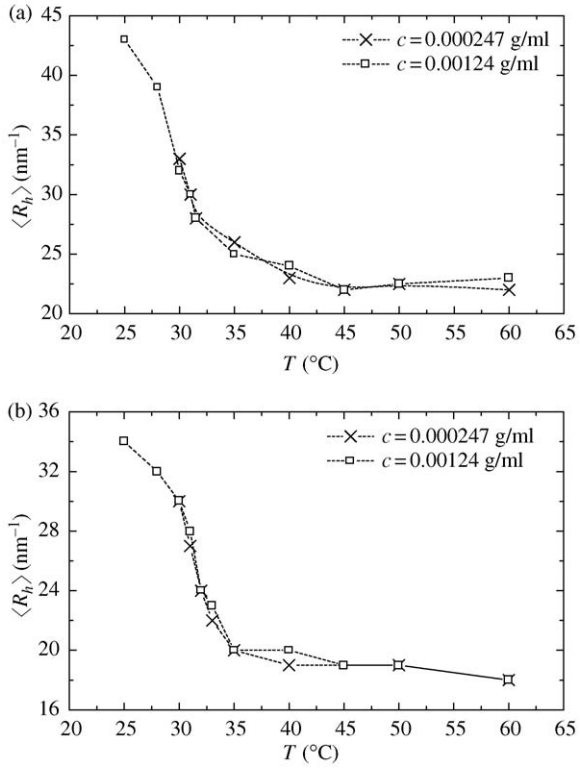

Figure 6 Temperature dependence of the average hydrodynamic radius $\langle R_h \rangle$ of PNIPAM-*b*-PEO-284 (a) and PNIPAM-*b*-PEO-398 (b) at two concentrations of 1.24×10^{-3} and 2.47×10^{-4} g/mL.

evident from the size distribution. Fig. 7 shows a $\langle R_h \rangle$ distribution of PNIPAM-*b*-PEO-398 at $c = 1.24 \times 10^{-3}$ g/ml. Even if the aqueous solution of PNIPAM-*b*-PEO-398 was kept under worse than θ-temperature of pure PNIPAM, 33 and 40 °C, respectively, for about 48 h, the $\langle R_h \rangle$ distributions at these two temperatures were not changed. It can accordingly be concluded that in the presence of BIS, the block copolymer nanoparticles with a well-defined core-shell structure are produced under the condition of higher feed molar ratios of NIPAM to PEO. The decrease in the average size, as shown in Fig. 6, is related to the temperature-induced collapse transition of PNIPAM cores of the individual core-shell nanoparticles.

The formation of a well-defined core-shell structure allows the PNIPAM cores to undergo the collapse transition without a perturbation of the aggregation in the entire range of temperature. The collapse transition of PNIPAM cores is continuous and broad. Even if there is a large amount of PEO, the collapse transition of PNIPAM cores almost completes under better than θ-temperature condition, similar to the collapse transition of interfacial PNIPAM chains with low molecular weights [23]. This phenomenon would be related to the segment concentration dependence of Flory–Huggins interaction parameter [24]. A further increase in the temperature can only lead to a compaction of collapsed PNIPAM globules in the cores.

It is worth noting that as the temperature is increased from 33 to 40 °C, the decrease in the average hydrodynamic radius is only about 3 nm but a broad and unsymmetrical distribution changes to a narrow and symmetrical one. The average hydrodynamic radii of single PNIPAM-*b*-PEO-398 nanoparticles are not as high as those of PNIPAM-*b*-PEO-284 both in good and in poor solvency conditions (see Fig. 6), even though the feed molar ratio of cross-linking agent BIS to NIPAM is identical for both samples during the copolymerization. This difference suggests that, under the above-mentioned synthetic conditions, the effective cross-linking density of PNIPAM cores in the single PNIPAM-*b*-PEO-284 nanoparticles is lower than that in the PNIPAM-*b*-PEO-398, which results in a higher degree of swelling at low temperatures and a loosely collapsed globule at high temperatures.

Fig. 8 shows the temperature dependence of $\langle R_h \rangle$ of PNIPAM-*b*-PEO-398 at $c = 3.92 \times 10^{-3}$ g/mL. This concentration was obtained by a slow evaporation of water from the dilute solution $c = 2.47 \times 10^{-4}$ g/mL at room temperature. Apparently, at the higher concentration, the change in the average size with temperature appears in a quite different fashion. It can be seen that $\langle R_h \rangle$ increases in the range 25–30 °C and then decreases with a further increase in temperature. There is no doubt that when the temperature is higher than 30 °C, the decrease in $\langle R_h \rangle$ should be attributed to the collapse transition of PNIPAM cores. However, unlike the more dilute solution of the same sample, the single PNIPAM-*b*-PEO-398 nanoparticles begin to undergo aggregation in the temperature range 26–30 °C, although the variation of the hydrodynamic radius still falls within the range of nanoscale. As discussed above, the single PNIPAM-*b*-PEO-398 nanoparticles have a well-defined core-shell structure with a hydrophilic PEO shell on the surfaces of a PNIPAM core. More importantly, the temperatures at

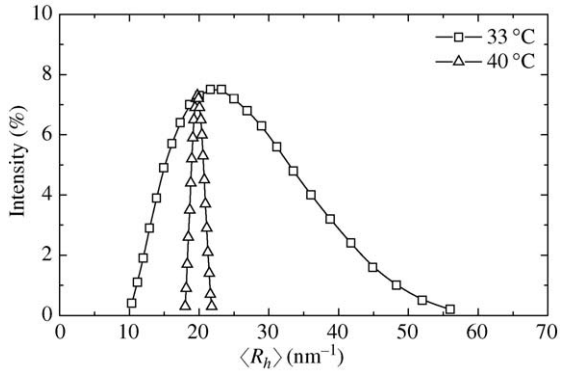

Figure 7 The average hydrodynamic radius distribution for PNIPAM-*b*-PEO-398 at $c = 1.24 \times 10^{-3}$ g/mL.

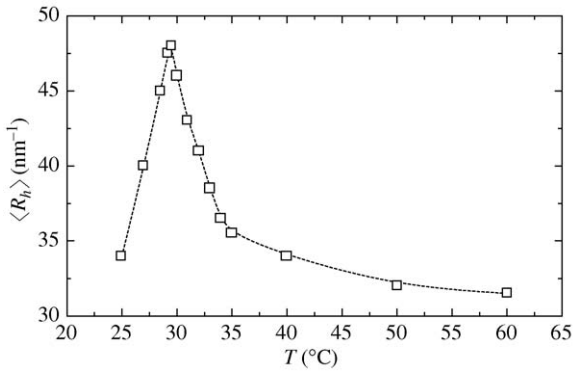

Figure 8 Temperature dependence of the average hydrodynamic radius $\langle R_h \rangle$ of PNIPAM-*b*-PEO-398 at $c = 3.92 \times 10^{-3}$ g/mL.

which larger values of $\langle R_h \rangle$ are obtained (see Fig. 8) are lower than the LCST of pure PNIPAM. Apparently, the driving force inducing the aggregation of PNIPAM-*b*-PEO-398 in the range of 26–30 °C should not be from the hydrophobic interaction between PNIPAM blocks. It is suggested that the increase in $\langle R_h \rangle$ in the range of 26–30 °C is due to the association between hydrophobic methyl groups at the periphery of PEO shells when the concentration of nanoparticles exceeds a certain value.

For many years, considerable effort has been devoted to understanding the association of aqueous solutions of linear polymers end-capped with hydrophobic groups [25, 26]. It is generally accepted that linear PEO chains with one and two hydrophobic end groups can self-assemble to form micelles and ''flowers'' [25, 26], respectively, with the variation of concentration or temperature. The association of hydrophobically modified PEO can been divided into several stages with the concentration [26]. At a very dilute concentration, the hydrophobic end groups of few polymer chains interact with each other and no large hydrophobic domains form. Hydrophobic domains consisting of a large number of hydrophobic end groups can be built-up at the critical micelle concentration (cmc), analogous to the case of low molecular weight surfactants. As the concentration is further increased to a so-called critical overlap concentration c^*, the aggregate particles formed can effectively interact with each other to form an infinite network structure.

Presumably, the above association mechanism described for the linear PEO chains with hydrophobic end groups can also be applied to the present system. The unique feature of the present system is that the association between hydrophobic methyl groups at the periphery of PEO shell brings together a number of thermosensitive core-shell nanoparticles. Physically, the critical concentrations defined for the aggregation process of linear polymers should not have the same meanings for the present system. The temperature may not induce the association of linear PEO chains with one methyl end group at the same concentration.

Fig. 9 shows schematically possible processes related to the temperature-induced association and collapse transition, respectively, of well-defined core-shell PNIPAM-*b*-PEO-398 nanoparticles. Since the PNIPAM cores in the core-shell nanoparticles undergo the contraction at lower temperatures (see Fig. 6), the formation of methyl group domains in the range 26–30 °C would be under kinetic constraints. In terms of the association of methyl groups at the periphery of PEO shells, the average size of aggregate particles would be a balance between an attraction force from the hydrophobic interaction of methyl groups and a repulsive force from the collapse transition of PNIPAM cores. Compared with the aggregate particles of PNIPAM-*b*-PEO-114 (see Figs. 3 and 5), the aggregate nanoparticles of PNIPAM-*b*-PEO-284 and PNIPAM-*b*-PEO-398 would contain a number of single core-shell nanoparticles and methyl group domains that are connected by PEO shells, as shown schematically in Fig. 9. The increase in temperature can bring about the collapse and compaction of PNIPAM cores but may not cause a significant change in the morphology of these aggregate nanoparticles.

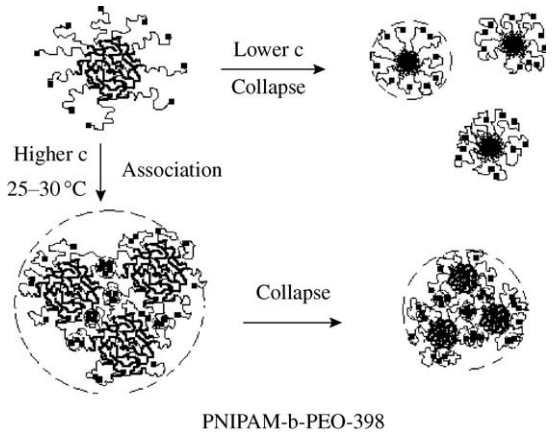

Figure 9 Schematic models for the coil-to-globule transition of PNIPAM cores in single PNIPAM-*b*-PEO-398 nanoparticles at low concentrations and the aggregation of single PNIPAM-*b*-PEO-398 nanoparticles due to the association of methyl groups at the periphery of PEO shells at high concentrations. Thin and bold curves represent PEO and PNIPAM, respectively. Filled squares represent methyl groups.

4. Conclusions

The effects of the feed molar ratio of NIPAM to PEO on the particle formation of PNIPAM-*b*-PEO in the presence of cross-linker BIS and their aggregation–collapse behavior have been studied. It is found that as the feed molar ratio of NIPAM to PEO is increased, the morphology of PNIPAM-*b*-PEO can be developed from grafting-like to a core-shell particle. When the feed molar ratio is high enough, e.g. $r = 284$ and 398 in the present work, individual PNIPAM-*b*-PEO nanoparticles with a well-defined core-shell structure can be obtained in the presence of BIS during the copolymerization. These nanoparticles comprises a hydrophobic PNIPAM core and a hydrophilic PEO shell with a large number of methyl groups at the periphery of the PEO shell. The low feed molar ratios of NIPAM to PEO, e.g. example $r = 34$, 57 and 114, can only produce grafting-like copolymers or hemispherical particles during the copolymerization. The stable aggregate particles can be obtained through an aggregation–collapse process with increasing temperature.

The feed molar ratio of NIPAM to PEO can significantly affect the aggregation–collapse behavior. At low concentration ($c = 1.24 \times 10^{-3}$ g/mL), the increase in temperature always induces the aggregation of grafting-like copolymers or hemispherical particles through the hydrophobic interaction between locally unshielded PNIPAM blocks, prior to the conformational transition of PNIPAM. When $r = 34$, individual aggregate particles would have a heterogeneous and incoherent structure in which there are a number of small domains of PNIPAM and methyl groups connected by PEO shells. These aggregate particles formed are filled with a large number of water molecules even at higher temperatures. When $r = 57$ and 114, the stable aggregate particles comprises a PNIPAM core and a PEO shell, although the possible interference of PEO blocks to the PNIPAM cores may be possible. Since the fraction of exposed PNIPAM blocks in PNIPAM-*b*-PEO-57 obtained is larger than that of PNIPAM-*b*-PEO-114,

greater numbers of collisions between PNIPAM-*b*-PEO-57 macromolecules are required for the formation of stable core-shell aggregate particles, which results in the larger size of PNIPAM-*b*-PEO-57 aggregate particles at higher temperatures. The competition between interchain aggregation and intrachain collapse cannot be detected when $r = 34$. Such a competition, however, manifests itself when $r = 57$ and becomes significant when $r = 114$.

However, at the same concentration, $c = 1.24 \times 10^{-3}$ g/mL, the PNIPAM cores in the single PNIPAM-*b*-PEO-284 and PNIPAM-*b*-PEO-398 nanoparticles obtained can undergo the ''coil-to-globule'' transition of PNIPAM cores within the range of temperature without the perturbation of aggregation. The PNIPAM cores have been effectively sterically stabilized by the PEO shells during the copolymerization. It is found that the PNIPAM-*b*-PEO-284 nanoparticles can swell to a larger degree than PNIPAM-*b*-PEO-398, which may be useful for optimizing the design of PNIPAM-*b*-PEO nanoparticles. The increase in the concentration of PNIPAM-*b*-PEO-284 and PNIPAM-*b*-PEO-398 nanoparticles can cause a weak association at temperatures lower than the θ-temperature of pure PNIPAM due to the hydrophobic interaction between methyl groups at the periphery of the PEO shells.

References

1. B. JEONG, Y. H. BAE, D. S. LEE and W. KIM, *Nature* **388** (1997) 860.
2. T. MIYATA, N. ASAMI and T. URAGAMI, *ibid.* **399** (1999) 766.
3. M. YAMATO, O. H. KWON, M. HIROSE, M. KIKUCHI and T. OKANOK, *Biomed. Mater. Res.* **55** (2000) 137.
4. D. LIANG, S. ZHIU, L. SONG, V. ZAITSEV and B. CHU, *Macromolecules* **32** (1999) 6326.
5. M. SHIBAYAMA and T. TANAKA, *Adv. Polym. Sci.* **109** (1993) 1.
6. H. G. SCHILD, *Prog. Polym. Sci.* **17** (1992) 163.
7. E. I. TIKTOPULO, V. N. UVERSKY, V. B. LUSHCHIK, S. I. KLENIN, V. E. BYCHKOVA and O. B. PTITSYN, *Macromolecules* **28** (1995) 7519.
8. G. CHEN and A. S. HOFFMAN, *Nature* **373** (1995) 49.
9. M. ANNAKA and T. TANAKA, *ibid.* **355** (1992) 430.
10. E. KOKUFUTA, Y. O. ZHANG and T. TANAKA, *ibid.* **351** (1991) 302.
11. Z. HU, X. ZHANG and Y. LI, *Science* **269** (1995) 525.
12. G. P. CHEN, Y. ITO and Y. IMANISH, *Biotechnol. Bioeng.* **53** (1997) 339.
13. S. JUODKAZIS, N. MUKAI, R. WAKAKI, A. YAMAGUCHI, S. MATSUO and H. MISAWA, *Nature* **408** (2000) 178.
14. M. D. C. TOPP, P. J. DIJKSTRA, H. TALSMA and J. FEIJEN, *Macromolecules* **30** (1997) 8518.
15. P. W. ZHU and D. H. NAPPER, *ibid.* **32** (1999) 2068.
16. R. PELTON, *Adv. Colloid Interf. Sci.* **85** (2000) 1.
17. W. F. POLIK and W. BURCHARD, *Macromolecules* **16** (1983) 978.
18. M. POLVERARI and T. G. M. VAN DER VEN, *J. Phys. Chem.* **100** (1996) 13687.
19. A. FARAONE, S. MAGAZU, G. MAISANO, P. MIGLIARDO, E. TETTAMANTI and V. VILLAR, *J. Chem. Phys.* **110** (1999) 1801.
20. X. QIU and C. WU, *Macromolecules* **30** (1997) 7921.
21. J. VIRTANEN and H. TENHU, *ibid.* **33** (2000) 5970.
22. D. H. NAPPER, in ''Polymeric Stabilization of Colloidal Dispersions'' (Academic, NewYork, 1983).
23. P. W. ZHU and D. H. NAPPER, *Colloids Surf.* **A113** (1996) 145.
24. V. A. BAULIN and A. HALPERIN, *Macromolecules* **35** (2002) 6432.
25. A. YEKTA, B. XU, J. DUHAMEL, H. ADIWIDJAJA and M. A. WINNIK, *ibid.* **28** (1995) 956.
26. E. BEAUDOIN, O. BORISOV, A. LAPP, L. BILLON, R. C. HIORNS and J. FRANCOIS, *ibid.* **35** (2002) 7436.

Received 11 July
and accepted 3 December 2003